Chewing mechanisms in the elderly investigated using Finite Element Modelling (FEM) for two soft cereal foods

M. Assad-Bustillos[1,2,3], S. Guessasma*[1], A.L. Reguerre[1], G. Della-Valle[1]

1. Biopolymères Interactions et Assemblages, INRA, Nantes, France
2. Centre des Sciences du Goût et de l'Alimentation, AgroSup Dijon, CNRS, INRA, Université Bourgogne Franche-Comté, Dijon, France
3. Cérélab®, Aiserey, France

*Corresponding author: sofiane.guessasma@inra.fr

Abstract

Cereal foods can be considered as cellular solids: texture is defined by their structure and mechanical properties. Elderly people show a significant alteration of oral health and salivation, causing difficulties to eat. Therefore, there is a need to understand chewing mechanisms of soft cereal foods in order to develop better food products that are fit for this population. In this context, the aim of this study is to understand and predict the mechanical changes of two ductile cereal food foams under conditions that mimic oral processing (compression loading). In this purpose, sponge-cake (SC) and brioche (B) were selected, and their mechanical properties were characterized under large compression levels (>90% in height reduction). Two distinct non-linear mechanical behaviors were observed: B showed plastic deformation and SC displayed hyper-elastic behavior. The apparent Young's modulus was higher for B (10kPa) than SC (5kPa). By using COMSOL® Multyphisics, 3D models of the homogenized cellular material and a unit cell were built using primitive shapes. Finite element computation was then used to derive the mechanical model representing the compressive response up to densification as compared to experimental data. Thanks to the development of a secant approach, the densification is modelled as a local increase in stiffness and implemented using an exponential function of the applied load. The mechanical response of both foods was approached.

These results are a first step towards a more accurate description of the mechanical and structural changes that occur during chewing in cereal soft foods and open prospect to reverse-engineering of foods with a desired mechanical response to compressive loading.

Keywords: Ductile foods, Mechanical properties, Compression, Densification, Elastic-plastic behavior, Hyper-elasticity, Food Oral Processing.

Introduction

Chewing is the first step of the eating process. Many complex mechanisms, take place to drastically transform food into a bolus that is ready to swallow[1]. Also, food oral processing is at the core of the sensory experience and pleasure that often comes with eating, since flavor and aroma are released at this stage[2]. The texture of foods is also an important feature responsible for likeability. Hence food mechanical properties play an important part in the chewing and bolus formation mechanisms, as well as perception [3]–[5]. Cereal foods can be considered as cellular solids, their texture is defined by their density, their cellular structure and the intrinsic mechanical properties of the wall materials [6]. Since chewing mechanisms often involve large deformations, high levels of stress and non-linear geometries, the use of Finite Element Models (FEM) may help to grasp the complexity of the problem. Indeed, FEM has been used before to calculate the stresses in the teeth, bones and muscles during chewing [7], [8]. Other related applications include modelling of fracture behavior and microstructure evolution of diverse materials for human and animal feeding [9]–[11].

However, one of the main difficulties of using FEM in food modeling under large strains is the complexity of the geometries involved, especially in cereal foods, given the high number of interconnections and contacts that can lead to convergence problems. Therefore, in the present work, by using COMSOL® Multiphysics, we have built simple geometries that represent the cellular material both explicitly (unit cell) and implicitly (homogenized

medium) of two ductile cereal foods. The idea was to derive the constitutive mechanical law for these two food products using a secant approach [12] that accurately represents their mechanical behavior under compressive loading up to 90% in height reduction. This work sets the basis for the development of models with a more realistic representation of the product microstructure, i.e. as captured by X-Ray micro-tomography.

Materials and Methods

Experimental Set-up

The mechanical properties of the studied foods were determined by uniaxial compression test. A circular steel cutter was used to prepare cylindrical samples with a diameter of 30 mm and a height of 30 mm. Both products were subjected to uniaxial compression using a universal testing machine equipped with a 1 kN load cell. The testing was performed with a cross head speed of 50 mm/min until 90% in height reduction between parallel plates. Five replicates were performed for each food sample. Results were expressed as engineering stress versus engineering strain plots, from which Young's modulus (E), and the critical stress (σ_{y0}), when applicable, were measured. E was calculated from the initial slope within the linear elastic domain, while σ_{y0} was defined as the stress value at the end of the linear domain.

Numerical Model

By using the Structural Mechanics module of COMSOL® Multiphysics v. 5.3, 3D models of the homogenized material and a unit cell were built using primitive shapes (Fig. 1). The first model is used to identify the compression behavior of the food products taken as homogenized materials up to the densification stage. The second model is used to retrieve the elasticity behavior of the same products taking into account the explicit porous structure. The second model is restricted to the linear elasticity domain because of difficulties to handle cell wall contact beyond the elasticity stage. The meshing of the models is performed using 3D structural tetrahedral elements. The typical meshes have 2557 domain elements and 508 boundary elements. Each element is described by four nodes, and each node has three degrees of freedom corresponding to displacements in the main space directions X, Y and Z. A linear elastic constitutive law with densification term was used for the sponge-cake (SC) food, and an elastic-plastic constitutive model was used for brioche (B), following Voce scheme for hardening rules.

For both models, Young's modulus was defined as an exponential stiffening function defined in [12] as follows:

$$E(\varepsilon\%)=E_0 + E_D \times \left(\frac{1-\exp(\frac{\varepsilon}{100})}{1-\exp(1)}\right)^d \quad (1)$$

where:

ε is the engineering strain, in % of height reduction;

E_0 and E_D are the initial Young's modulus and the densification modulus; and

d is the stiffening coefficient at densification

For both products, equation (1) takes into account the stiffening of the material during loading due to the increase of cell wall contact. Equation (1) uses the principle of superposition of elasticity terms. In addition, plasticity is accounted for in the case of product B using the following equation assuming an isotropic hardening rule of the form

$$\sigma_Y = \sigma_{Y0} + \sigma_S\left(1 - exp\left[-\beta\varepsilon_p\right]\right) \quad (2)$$

where:

σ_{Y0} is the yield stress

σ_S is the saturation flow stress

β is the saturation exponent

ε_p is the plasticity strain, which is defined as

$$\varepsilon_p = \varepsilon_t - \varepsilon_e \quad (3)$$

where:

ε_t and ε_e are the total and elasticity strains.

Moreover, by using the parametric sweep functionality, the set of values of the densification modulus (E_D) and the stiffening coefficient (d) that fit the best the experimental data were approached.
For each geometry, the same boundary conditions are implemented. These correspond to a compression loading under unlubricated conditions: all degrees of freedom are grounded for all nodes belonging to the bottom surface (UX=UY=UZ=0 for Z=0). All homologue nodes at the opposite surface are constrained for motion in Z-direction (UX=UY=0, UZ=U<0, where U is proportional to the reduction in height). The loading was defined as proportional to the desired strain level. A stationary study was then conducted, and the auxiliary parameter sweep function allowed the computing of the study for 5 different consecutive strain values from 0 to 90 % for the homogenized model, and 0 to 1% for the unit cell.

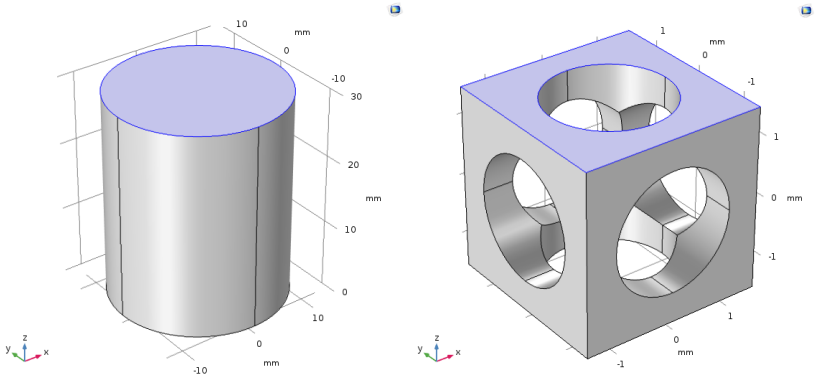

Figure 1. Geometries represeting the homogeneized material (left) and a unit-cell (right) built with COMSOL®. The highlighted surfaces indicate the loading surface.

Results and Discussion

Experimental Results

Figure 2 compares the compression behavior of the two studied products. A typical behavior of ductile cellular material with three stages is depicted for both products. The first stage is a linear branch corresponding to the elasticity part of the cellular material behavior. Because of the significance of the airy structure (porosity content of 67% for product B against 79% for product SC), the slope is limited and it appears like both products exhibit a rubbery-like behavior. The measured Young's moduli are 20±3 and 5±1 kPa for product B and SC, respectively. Some differences appear at the second stage, which corresponds to the cell collapse plateau. Product B seems to develop stress saturation trend that can be approached using a plasticity model. The width of the cell collapse plateau is 65% and 71% for product B and SC before reaching the densification stage. Figure 2 demonstrates that there are marked differences between the studied products in terms of stress magnitudes but also in terms of type of behavior. In order to better quantify these differences, the finite element results are explored to determine the type of constitutive law that represents better both products.

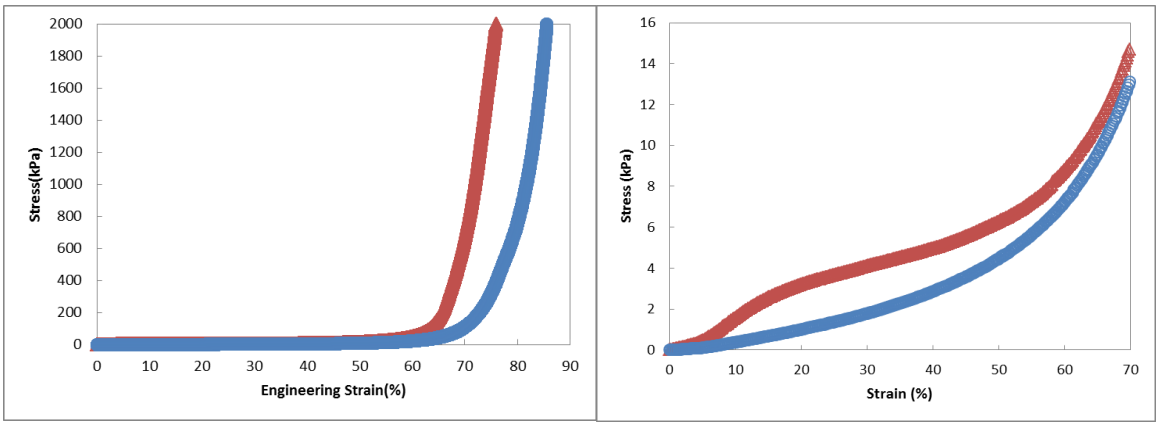

Figure 2. Experimental stress vs strain responses of Brioche (red) and Sponge-cake (blue). On the left, the whole curve up to 90% of strain; on the right, a zoom of the first part to show the characteristic mechanical behaviors.

Simulation Results

A sensitivity analysis is conducted to predict the influence of the densification term in the constitutive model on the compression response. Figure 3 illustrates the variation of the stiffening parameters for the simulation of the compression behavior of product SC, where d represents the % of strain that is needed for densification; and the E_D value represents the stress rate at densification. Within the range (0 – 4), the stiffening coefficient d is found to control both the slope of the densification stage and the width of the cell collapse plateau. The higher the value of d, the more reduction in height is needed for densification to begin. This parameter captures thus the effect of material density as this is the structural attribute that allows a more or less rapid densification. The densification modulus is the second parameter, which is varied in a large range, typically between 0.5 MPa and 0.5 GPa. The E_D value represents the stress rate at densification. Therefore, the higher the value of $E_{D,}$ the faster the stress will increase during the densification stage. The two terms are complementary parameters to capture the densification tendencies of the two products.

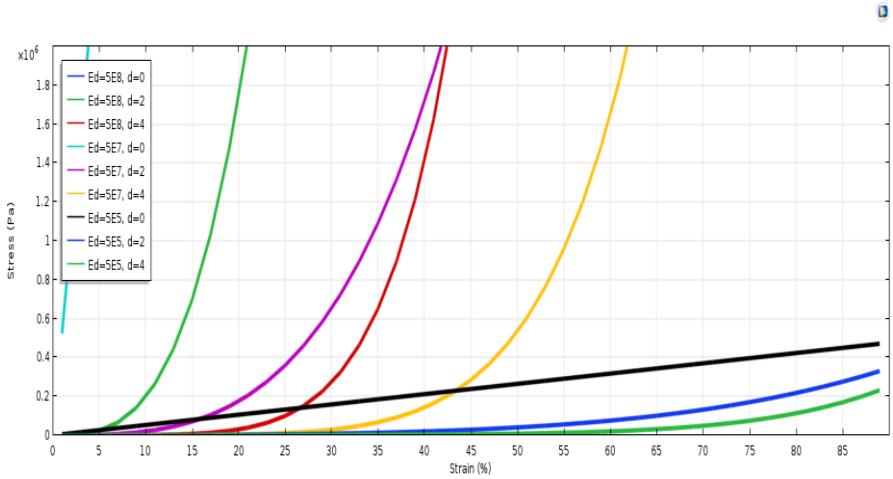

Figure 3. Sensitivity analysis showing the effect of the densification terms on the compression response of a homogeneized cellular structure for the product SC.

Figure 4 compares the experiemntal and numerical results based on the homogeneised cellular material for the two products. For each simulation, the parameters of the model that best fit the experimental data (Fig. 1) are shown in Table 1. These were identified through a parametric sweep for the homogenized models. It is found that product SC exhibits a hyperelastic behaviour well captured by the constitutive law that involves a densification term.

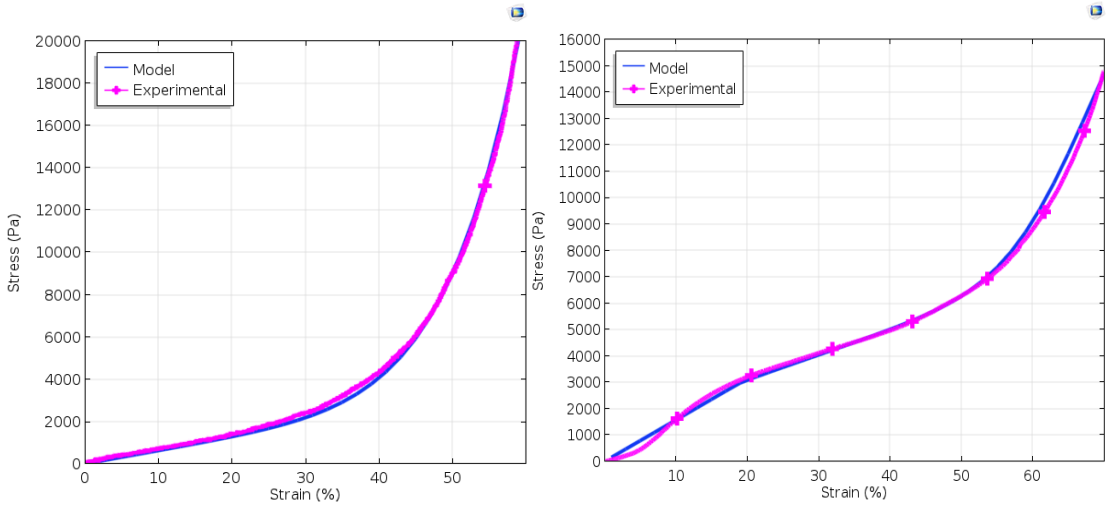

Figure 4. Comparison between the experimental compression behaviour of product (left) SC and (right) B against the homogenized material models including the proposed stiffening term.

The second product, however, displays a non negligeable plasticity stage that is handelled by the plasticity term in the constitutive model. Indeed, a high sensitivity of the product's response to both saturation exponent and flow stress is predicted. Only minor differences are found between the model and the experimental evidence. This difference is mainly explained by the unhomogeneous contact between the sample and the compression plates at the first load levels that results in the cruve tail depicted in figure 4.

Model parameters	Sponge-cake(SC)	Brioche (B)
$\mathbf{E_0}$	5 kPa	20 kPa
$\mathbf{E_D}$	0.55 MPa	4 MPa
d	4	8
$\boldsymbol{\beta}$	-	$1.5x10^{-2}$
$\boldsymbol{\sigma_{y0}}$	-	3 kPa
$\boldsymbol{\sigma_s}$	-	14 MPa

Table 1. Summary of the parameters used for all simulations.

Finally, by using the same model parameters identified in Table 1, the unit cell models were implemented for both products. These models are meant to represent the porosity of each material, and therefore their density values (0.21 and 0.33 g/cm^3 for SC and B, respectively) were added to the model. However, as already mentioned, since such models cannot handle high levels of strain, a height reduction of 1% was applied. The resulting stress fields for both the homogenized and unit cell models are shown in Figure 5.

The distribution of the normal stress component σ_{zz}, where z is the loading direction for both models is determined for a 1% of reduction in height.

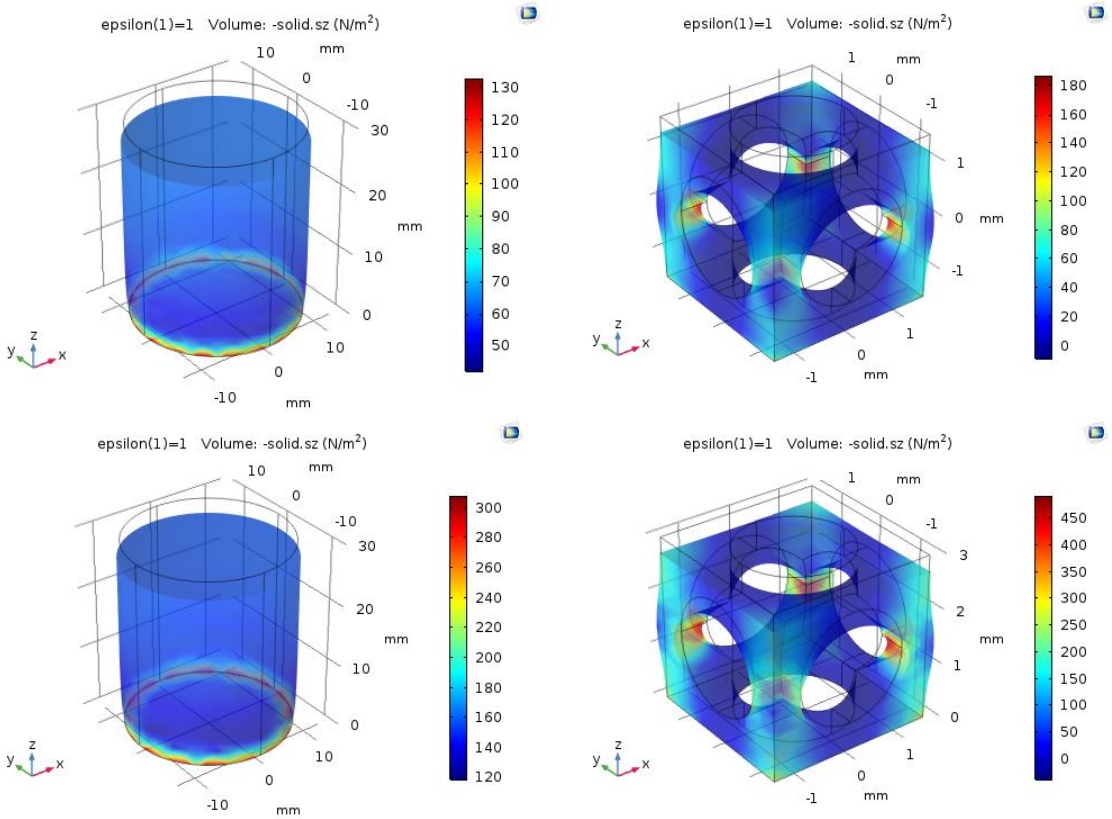

Figure 5. Stress component σ_{zz} distribution of product SC (top) and B (bottom), for a reduction by 1% of the total height (left) homogeneized model, (right) unit cell model.

The unit cell model (on the right) shows that bending of cell walls is the leading deformation mechanism, which is attested by the stress localization depicted at mid-height. Generally speaking, the typical compression behavior of a cellular material is a combination between uniaxial deformation and bending deformation mechanisms. If the local density of material is large, then uniaxial deformation prevails. In the present case, the large porosity

content of both products promotes bending as a predominant deformation mechanism. As a consequence, there cell wall contact at mid-height is expected after the linear elasticity stage, which cannot be accurately modelled without the use of proper contact elements. The model on the right considers the effect of cell wall contact by modifying the stiffness of the material depending on the load level. The stress component counterplot shows that the regions of higher stress are those generated at the contact between the cellular material and the compression stages. Stresses as large as 0.13 kPa are reached for 1% of height reduction. With regards to the experimental results (Figure 2), these levels are coherent with the stress levels in the elasticity stage.

Conclusions and Prospects

The modelling of the hyper-elasticity of food products using secant approach proved to be an effective way to derive the compression behavior up to the densification stage. Only one product exhibited such a behavior. The model remarkably captures all the deformation stages with a limited number of mechanical parameters. The combination of plasticity and densification terms requires a deeper analysis as there is a more complex interdependency between the parameters associated with these two terms to fully capture the behavior of the second product. This last one exhibited an elastic-plastic-densification response requiring the tuning of a larger number of parameters. Finally, the modelling of mechanical response of the cellular structure of the two foods under compression using high resolution ultra-fast x-ray micro-tomography is currently under investigation to retrieve the role of local rearrangement of the cellular structure during loading. The resulting 3D images will provide useful information in order to better capture the evolving cell contacts and improve the current models developed using COMSOL®.

These results are a first step towards a more accurate description of the mechanical and structural changes that occur during chewing in cereal soft foods and open prospect to reverse-engineering of foods with a desired mechanical response to compressive loading.

Acknowledgements

This work was supported by AlimaSSenS project (ANR-14-CE20-0003).

References

[1] J. F. Prinz and P. W. Lucas, “An optimization model for mastication and swallowing in mammals,” *Proc. R. Soc. London B Biol. Sci.*, vol. 264, no. 1389, 1997.

[2] C. Salles *et al.*, “In-mouth mechanisms leading to flavor release and perception.,” *Crit. Rev. Food Sci. Nutr.*, vol. 51, no. 1, pp. 67–90, 2011.

[3] T. Witt and J. R. Stokes, “Physics of food structure breakdown and bolus formation during oral processing of hard and soft solids,” *Curr. Opin. Food Sci.*, vol. 3, pp. 110–117, 2015.

[4] J. Gao, Y. Wang, Z. Dong, and W. Zhou, “Structural and mechanical characteristics of bread and their impact on oral processing: a review,” *Int. J. Food Sci. Technol.*, pp. 1–15, 2017.

[5] Y. Pascua, H. Koç, and E. A. Foegeding, “Food structure: Roles of mechanical properties and oral processing in determining sensory texture of soft materials,” *Curr. Opin. Colloid Interface Sci.*, vol. 18, no. 4, pp. 324–333, 2013.

[6] G. E. Attenburrow, R. M. Goodband, L. J. Taylor, and P. J. Lillford, “Structure, mechanics and texture of a food sponge,” *J. Cereal Sci.*, vol. 9, no. 1, p. IN1-70, 1989.

[7] B. Dejak, A. Młotkowski, and M. Romanowicz, “Finite element analysis of stresses in molars during clenching and mastication.,” *J. Prosthet. Dent.*, vol. 90, no. 6, pp. 591–7, Dec. 2003.

[8] M. A. Berthaume, E. R. Dumont, L. R. Godfrey, and I. R. Grosse, “The effects of relative food item size on optimal tooth cusp sharpness during brittle food item processing.,” *J. R. Soc. Interface*, vol. 11, no. 101, p. 20140965, Dec. 2014.

[9] C. G. Skamniotis, M. Elliott, and M. N. Charalambides, “On modeling the large strain fracture behaviour of soft viscous foods,” *Phys. Fluids*, vol. 29, no. 12, 2017.

[10] S. Guessasma and L. Hedjazi, “On the fragmentation of airy cereal products exhibiting a cellular structure: Mechanical characterisation and 3D finite element computation,” *Food Res. Int.*, vol. 49, no. 1, pp. 242–252, 2012.

[11] I. K. Mohammed, M. N. Charalambides, J. G. Williams, and J. Rasburn, “Modelling

deformation and fracture in confectionery wafers," *Procedia Food Sci.*, vol. 1, pp. 499–504, Jan. 2011.

[12] S. Guessasma and H. Nouri, "Comprehensive study of biopolymer foam compression up to densification using X-ray micro-tomography and finite element computation," *Eur. Polym. J.*, vol. 72, pp. 140–148, 2015.